

Compressive Sensing based Continuous ECG Monitoring and Processing using a Novel Feature Extraction Algorithm

Meenu Rani, S. B. Dhok, R. B. Deshmukh and Vinay Kumar

Visvesvaraya National Institute of Technology, Nagpur, India-440010.

Abstract: The electrocardiogram (ECG) represents the electrical activity of heart. This activity is monitored to check, whether, heart is functioning normally or not. For this purpose, the acquisition of ECG signal is usually done at Nyquist Rate. This generates too many samples and invokes the need of compression before storage and transmission. In this scenario, compressive sensing (CS) has been proved to be a better candidate. CS being a newer sensing modality, which, samples the signals at a rate much below the Nyquist rate and still allows faithful reconstruction from fewer samples. In this work, a CS acquisition strategy, namely, the random demodulator (RD) has been used for the acquisition of ECG signal, to overcome the storage and transmission overhead in continuous ECG monitoring. At the receiver end, reconstruction is tried from the received compressive measurements using several CS reconstruction algorithms from convex and greedy approaches. In order to identify a better CS reconstruction algorithm for ECG signal, the reconstruction performance of these algorithms is compared using parameters like undersampling ratio, speed and accuracy of reconstruction. From the reconstructed ECG signal, the disease classification has been done by extracting its features with the help of proposed feature extraction algorithm. To validate the universality of proposed algorithm for ECG signals, the algorithm has been tested on several data sets of ECG signal, which are taken from MIT-BIH database. Finally, the robustness analysis of 'CS for ECG monitoring' has been done by investigating on information security and denoising aspects.

Keywords: Compressive Sensing, ECG-monitoring, random demodulator, convex optimization, greedy algorithms, Feature Extraction.

I. Introduction

Requirement of continuous electrocardiogram (ECG) signal monitoring for early detection of disease poses certain challenges on traditional signal acquisition techniques. ECG signals possesses very low activity and remains idle for most of the duration. For faithful reconstruction, sampling such signals by conventional methods results in huge amount of samples and hence compression is mandatory before storage and transmission. Recently, a rapid growth has been reported in the area of remote health care, in which health is monitored remotely using battery operated devices. Longer battery life is major requirement of these systems for continuous monitoring. But, for error free operation, signal must be oversampled, which consumes a considerable amount of power. As a consequence of oversampling, the huge amount of samples are generated, that needs to be compressed. This requires extra processing power. In such situation, compressive sensing (CS) proves itself to be a better candidate in overcoming

the disadvantages of conventional methods. The acquisition schemes offered by CS, sample a signal at much lower rate. Hence, by generating far fewer samples, CS avoids need of compression, thereby lowering the power consumption [20]–[24].

CS is an emerging signal processing technique, introduced in 2004 by Donoho, Candès, Romberg and Tao [1], [2]. These researchers developed the mathematical foundation of CS and demonstrated its applicability for sparse or compressible signals. Sparse signals are those, which can be represented by using fewer significant components, compared to the total length of signal. Similarly, if the sorted components of a signal decay rapidly obeying power law, then the signals are called compressible signals. In CS paradigm, the sampling rate of a signal is dependent on the sparsity of underlying signal and is independent of the frequency of the highest frequency component present in the signal. CS utilizes random sampling mechanism for sampling signals at a very low rate and hence generating far fewer random samples, which can be easily stored or transmitted. This mechanism gives an impression of compressing the signal at the time of sampling/sensing and hence the name ‘compressive sensing’. At the receiver end, the original signal can be reconstructed by the nonlinear techniques, which are more complex than the conventional techniques. Therefore, it can be said that CS shifts the complexity of signal processing from acquisition end to the reconstruction end [3]–[5].

CS is advantageous over conventional sampling technique, specifically, in cases where, the number of measurements that can be taken are limited because of factors like cost, speed, power, etc. Examples of such prominent areas where CS finds its application are medical imaging, ultrawideband communication, seismology, telemonitoring, etc. In this regard, an early prototype hardware implementation by Duarte *et al.*, is the ‘single pixel camera’, which demonstrates the image acquisition using CS with a single photodiode [11]. Other implementations for signal acquisition using CS are: random demodulator (RD) for wideband signals [12], modulated wideband converter (MWC) for multiband wideband signals [13], compressive multiplexer for ultrawideband signals [14], etc. [15]. In this paper, RD has been used for simultaneous acquisition and compression of ECG signal, because of its simple architecture. The acquisition is then followed by reconstruction using popular CS reconstruction approaches.

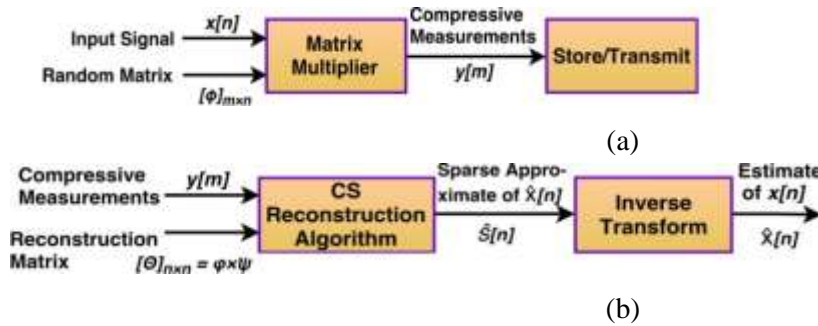


Figure 1. Mathematical model of CS: (a) acquisition model, (b) reconstruction model.

Contribution: The major contributions of this work are: i). comparison of sparsifying basis for ECG signal, ii). performance comparison of CS reconstruction algorithms to identify a better performing algorithm, iii). a universal feature extraction algorithm for extracting features from ECG signal for the purpose of disease classification. At last, the robustness analysis of CS based ECG monitoring has been done by investigating on denoising and information security aspects.

The organization of this paper is as follows: section II presents the preliminaries and mathematical model of CS. Section III, describes the acquisition of ECG signal using RD technique of CS. Section IV, is about the reconstruction methods used in this paper for recovering the original signal back from compressive random measurements. A performance comparison of popular CS reconstruction methods is also presented to identify a better performing algorithm for ECG signal reconstruction. In section V, a novel feature extraction algorithm is proposed to extract features from different types of ECG signals. The analysis done to test performance of this algorithm is also presented along with the disease classification done using the extracted features. Section VI, discusses the robustness analysis of CS for ECG monitoring.

II. Preliminaries and mathematical model of CS

A. Acquisition Model

CS is different from traditional methods in the way it samples signals. CS works by taking fewer random measurements. The measurements are non-adaptive, *i.e.*, not learning from previous measurements. To further reduced number of measurements required for perfect reconstruction, the choice of signal sparsity domain and acquisition domain should be such that both the domains are incoherent from each other. For example, time and frequency domains are incoherent in the sense that a signal having sparse representation in frequency domain, spreads out in time domain and vice versa. Similarly, spikes and sines are incoherent from each other. The random acquisition method of CS can be mathematically described by (1) and is shown in Fig.1(a).

$$y = \varphi x, \tag{1}$$

where, $x \in \mathbb{R}^n$ or \mathbb{C}^n is input signal of length n , $\varphi \in \mathbb{R}^{m \times n}$ or $\mathbb{C}^{m \times n}$ is an $m \times n$ random measurement matrix and $y \in \mathbb{R}^m$ or \mathbb{C}^m is the measurement vector of length m . Here, the number of measurements is much less than the length of input signal, *i.e.*, $m \ll n$ [3]–[5].

TABLE I: DEFINITIONS OF VARIOUS NORMS USED THROUGHOUT.

Norm	Definition	Comments
ℓ_p	$\ x\ _p = \sqrt[p]{\sum_i x_i ^p}$	General definition of a norm.
ℓ_0	$\ x\ _0 = \#(i: x_i \neq 0)$	A pseudonorm, which gives number of non-zero elements in a vector.
ℓ_1	$\ x\ _1 = \sum_i x_i $	It gives the absolute sum of elements of a vector.
ℓ_2	$\ x\ _2 = \sqrt{\sum_i x_i ^2}$	Euclidean norm: length or size of a vector

B. Reconstruction Model

The CS reconstruction model is shown in Fig.1(b). The input arguments to the CS reconstruction algorithm are y and Θ , where matrix $\Theta = \varphi \times \psi \in \mathbb{R}^{m \times n}$ or $\mathbb{C}^{m \times n}$ is the CS reconstruction matrix and ψ

is the sparsifying basis of the signal x . The sparsifying basis is the basis in which signal has sparse representation. Using this sparsifying basis, the signal can be written as a linear combination of its basis vectors, *i.e.*, columns of ψ , as given by (2).

$$x = \sum_{i=1}^n s_i \psi_i = \psi s, \quad (2)$$

where, $s \in \mathbb{R}^n$, is the sparse coefficient vector of length n , having fewer significant/nonzero entries. Using vector y and matrix Θ as inputs, the CS reconstruction solves an inverse problem to find the solution of (1), to recover original signal back from compressive measurements. This inverse problem is an underdetermined system of linear equations having infinite number of solutions. However, it has been shown in literature that (1) can be solved uniquely, by posing it as an ℓ_0 -optimization problem, as given by (3). Subject to some constraints, the ℓ_0 -optimization tries to find a solution having minimum ℓ_0 -norm. This is equivalent to trying all the possibilities to find the desired solution [3]–[5].

$$\hat{s} = \underset{s}{\operatorname{argmin}} \|s\|_0 \quad \text{subject to } \Theta s = y, \quad (3)$$

where, \hat{s} , is the estimate of s and $\|s\|_0$ denotes the ℓ_0 -norm of s and is defined in Table I. Also, the definitions of other norms that are used throughout the manuscript, are given in Table I [7]. Searching for a solution of (3) by trying all possible combinations, is a computationally extensive exercise, even for a medium sized problem. Hence, ℓ_0 -minimization problem has been declared as NP-hard. Alternates have been proposed in literature, which are capable of obtaining a solution similar to the ℓ_0 -minimization for the above problem, in near polynomial time. One of the options is to use convex optimization and searching for a solution having minimum ℓ_1 -norm, as given by (4).

$$\hat{s} = \underset{s}{\operatorname{argmin}} \|s\|_1 \quad \text{subject to } \Theta s = y, \quad (4)$$

where, \hat{s} , is the estimate of s and $\|s\|_1$ denotes the ℓ_1 -norm of s . The solution to convex optimization problems can be obtained with the help of solvers available from linear programming, such as, simplex method, interior point algorithm, etc. The output of CS reconstruction algorithm is the sparse vector, \hat{s} , from which, estimate, \hat{x} , can be obtained by taking inverse transform [9], [10], [16].

C. Necessary and Sufficient Conditions for perfect Recovery

1) *Restricted Isometry Property (RIP)*: The necessary condition for perfectly recovering s from compressive measurements y is that the reconstruction matrix Θ must obey RIP of order k , as given by (5).

$$1 - \delta \leq \frac{\|\Theta v\|_2}{\|v\|_2} \leq 1 + \delta, \quad (5)$$

where, k is the sparsity of vector s , v is a vector having same k -nonzero entries as s and $\delta > 0$ is called restricted isometry constant. This inequality states that the matrix Θ must preserve the distance between two k -sparse vectors, so that, every k -sparse solution can be identified uniquely. However, the condition is not sufficient for a stable solution. The sufficient condition is that the matrix Θ must satisfy (5) for an arbitrary $3k$ -sparse vector v . Although this condition is both necessary and sufficient, but the difficulty lies in the calculation of δ which, itself is a very tough task. So, another simpler condition, which guarantees stable solution is incoherence, as described below [4], [5].

2) *Incoherence*: This condition states that the two bases, *i.e.*, the measurement bases φ and sparsifying basis ψ , must be incoherent from each other. This enables each measurement to capture some part of information present in the signal. Lower value of coherence is desired, which in turn, lowers the

number of measurements required for CS reconstruction. The relation between coherence and number of measurements required for faithful reconstruction, is given by (6).

$$m \geq c\mu^2 k \log n, \quad (6)$$

where, m is the number of measurements, c is a constant and μ is the coherence between two matrices. The coherence is calculated by the largest correlation between elements of two matrices, as given by (7).

$$\mu(\varphi, \psi) = \sqrt{n} \cdot \max_{1 \leq i, j \leq n} |\langle \varphi_i, \psi_j \rangle|, \quad (7)$$

where, $|\langle \cdot, \cdot \rangle|$ represents the inner product operator. The range of coherence is $\mu(\varphi, \psi) \in [1, \sqrt{n}]$. The widely used measurement bases in CS are the random measurement matrices, which are drawn from Gaussian or Bernoulli distributions. The random matrices are incoherent with any sparsifying basis used and they also satisfy the RIP property. Another random measurement basis used are the partial Fourier matrices, which are obtained from Fourier matrices, by randomly selecting its rows [4]–[6]. Recently, structured matrices like, toeplitz and circulant matrices have also been proposed as good CS matrices. These matrices are shown to have performance comparable to random matrices. The advantages of these matrices over random matrices are: easy storage and reproducibility at reconstruction end, which in turn, lowers the transmission overhead [19].

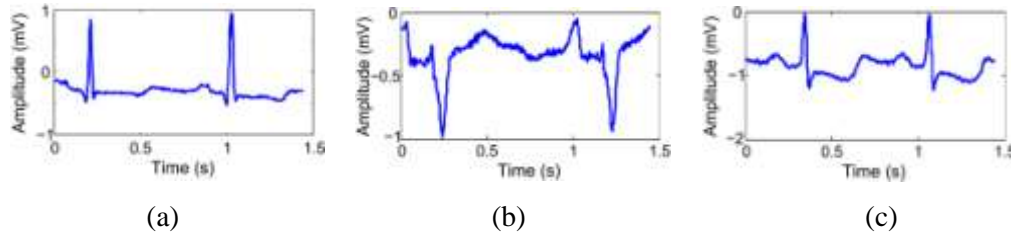


Figure. 2. Different categories of ECG signals taken from MIT-BIH database: (a) data set 100, (b) data set 108, (c) data set 112.

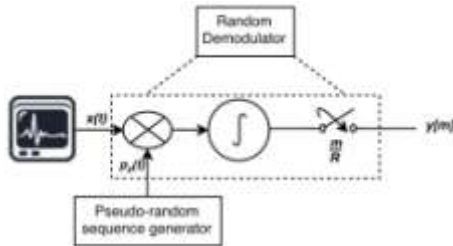


Figure. 3. Acquisition of ECG signal based on CS technique, the random demodulator.

III. CS Based ECG Signal Acquisition

The ECG data sets used in this paper are taken from MIT-BIH database. For processing these signals, the techniques that are used and proposed in this paper, have been tested on several ECG data sets. As the results for all the ECG data sets cannot be presented here, so some specific ECG data sets, representing a particular category of ECG signal, have been selected and the corresponding results have been presented in this paper. All the processing has been done using MATLAB 2015a, running on a 2.4 GHz Intel core i3-3110M, windows 10 pro based system with 4 GB RAM.

The selected ECG signals belongs to data sets 100, 108 and 112, and are shown in Fig.2(a), Fig.2(b) and Fig.2(c), respectively. These signals are sampled using RD technique of CS to obtain the compressive measurements, as shown in Fig.3. The first stage of RD is a multiplier, which, multiplies the input ECG signal by a pseudo-random chipping sequence of ± 1 s. This introduces randomness in the input signal and smear its frequency contents in lower frequency band. To retain the lower frequencies, this signal is then passed through an integrator, serving as a low pass filter. Now, the integrator output is sampled at a rate, which is much lower compared to sampling rate required by conventional technique [12].

The matrix form of RD is governed by (8) and (9). In case of undersampling by a factor of 2, the experimental settings done for ECG signal acquisition using CS are $n = 520$ and $m = 260$. This implies, the input ECG signal x is a vector of size 520×1 , measurement matrix $\varphi = H \times P$ is of size 260×512 and output vector y is of 260×1 . Here, P is a 520×520 diagonal

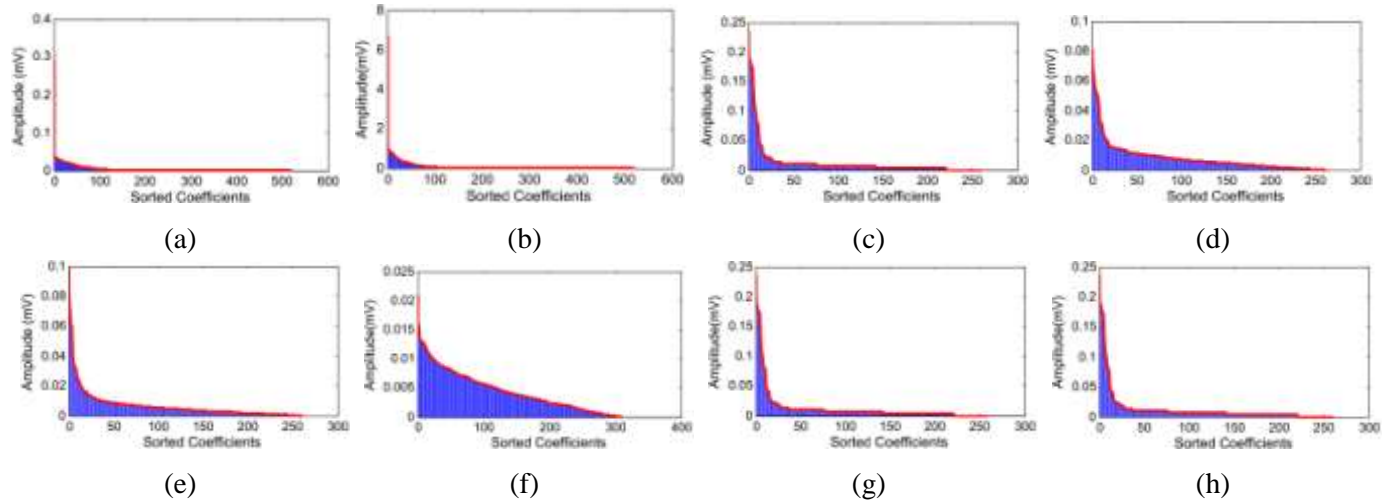


Figure. 4. Sparsity test for ECG signal using: (a) Fourier transform, (b) DCT, (c) Haar wavelet transform, (d) Coiflet wavelet transform, (e) Symlet wavelet transform, (f) discrete Meyer wavelet transform, (g) biorthogonal wavelet transform and (h) reverse biorthogonal wavelet transform.

matrix of chipping sequence, having diagonal elements as pseudorandom sequence $p_c(t)$ of ± 1 s and H is 260×512 accumulate and dump matrix serving as integrator. The number of terms to be accumulated for one measurement are given by $R = \lfloor (n/m) \rfloor$.

$$P = \begin{bmatrix} p_1 & & \\ & \ddots & \\ & & p_n \end{bmatrix}; \quad H = \begin{bmatrix} 111 \dots & & \\ & 111 \dots & \\ & & 111 \dots \end{bmatrix} \quad (8)$$

$$\left. \begin{aligned} \tilde{x} &= Px \\ y &= H\tilde{x} = \varphi x \\ \varphi &= HP \end{aligned} \right\} \quad (9)$$

An example of RD matrices for $n = 8$ and $m = 4$ is given in (10), (11) and (12).

minimum l_1 -norm, subject to the equality constraint $\Theta s = y$. BP works well if, the measurements are noiseless.

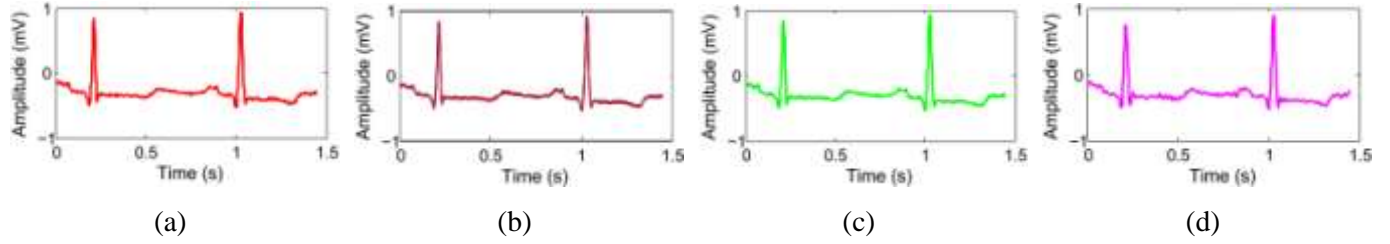


Figure. 5. CS reconstruction results for ECG signal data set 100, for an undersampling factor of 2, using algorithms: (a) BP, (b) BPDN, (c) OMP and (d) CoSaMP.

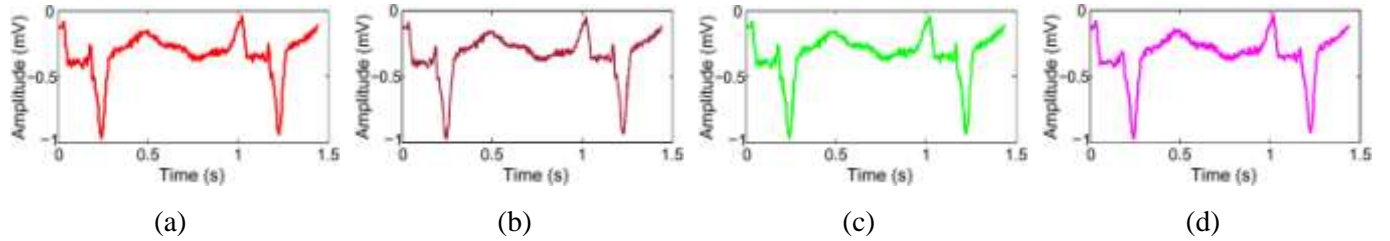


Figure. 6. CS reconstruction results for ECG signal data set 108, for an undersampling factor of 2, using algorithms: (a) BP, (b) BPDN, (c) OMP and (d) CoSaMP.

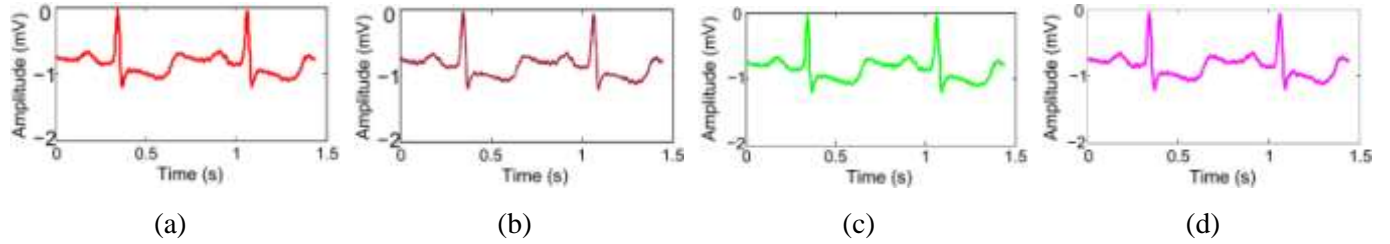


Figure. 7. CS reconstruction results for ECG signal data set 112, for an undersampling factor of 2, using algorithms: (a) BP, (b) BPDN, (c) OMP and (d) CoSaMP

- *BPDN*: BPDN was also proposed by S. Chen *et al.*, in 1999 [16]. When the measurements are contaminated by noise, then to suppress noise, BPDN uses a relaxed condition on constraint. BPDN finds a solution having minimum l_1 -norm, subject to the quadratic inequality constraint given by (13).

$$\hat{s} = \underset{s}{\operatorname{argmin}} \|s\|_1; \quad \text{subject to} \quad \frac{1}{2} \|y - \Theta s\|_2^2 \leq \epsilon, \quad (13)$$

The optimization problems described above, can be solved by algorithms like: simplex method, interior point method from linear programming [16]. The basic steps of one of the solver, named, interior point method are described below:

- The algorithm begins with a non-sparse initial solution, which lies in the interior of simplex. Here, the simplex is a convex polyhedron formed by connecting the set of all feasible solutions or points.
- Then, transformations are applied to sparsify the solution. This moves the solution inside the simplex in a direction to reach the vertex of simplex.

iii). Repeat step ii), until a solution is reached, which has n or less than n significant entries. The result so obtained, corresponds to a vertex of the simplex.

2) *Greedy Approach*: Greedy algorithms are relatively simpler and faster than convex optimization methods. In this experimentation, two algorithms corresponding to two versions of greedy algorithms, *i.e.*, serial and parallel have been used.

TABLE II. THE OMP ALGORITHM.

Step	Operation
1.	initialization $r_0 = y, \hat{s}_0 = \emptyset, \Lambda_0 = \emptyset, i = 1$
2.	Atom Search $C_i = \Theta^T r_{i-1}, \theta_i = \underset{j}{\operatorname{argmax}} (C_i)_j , \Lambda_i = \Lambda_{i-1} \cup \theta_i$
3.	Update Solution $\hat{s}_i = \underset{s}{\operatorname{argmin}} \ (y - \Theta_{\Lambda_i} s) \ _2^2 \quad (\text{Least Square})$
4.	Update Residual $r_i = r_{i-1} - \Theta_{\Lambda_i} \hat{s}_i, \quad i = i + 1$
5.	if $\ r_i \ _2 \leq \epsilon$, stop, otherwise go to step 2.

- *OMP Algorithm*: OMP is a serial greedy algorithm, proposed by Y. C. Pati *et al.*, in 1993 [17]. The basic steps of OMP algorithm are described below and are shown in Table II.

i). The residual vector r is initialized to measurement vector y . Solution vector \hat{s} and index set Λ are initialized to null vector. Iteration counter i is initialized to 1.

ii). The atom search step finds a column of Θ , that is maximally correlation with r , where, Θ^T is the transpose of matrix Θ . The index set Λ is then updated with the position of selected atom.

iii). Using the selected atoms of Θ , the solution \hat{s}_i is updated using least square method. Least square is used in OMP to find a solution, which, best fits the subspace spanned by the selected atoms of Θ .

iv). The residual vector is then updated using the current solution. These steps are repeated either k times or until residual becomes lesser than certain threshold [17].

- *CoSaMP Algorithm*: CoSaMP is a parallel greedy algorithm, proposed by Needell and Tropp in 2009 [18]. Different from OMP, CoSaMP selects $2k$ maximally correlated atoms in each iteration. These atoms are then added with atoms selected in previous iteration. From these, the best k atoms are retained for least square step to obtain sparse solution vector \hat{s} and the process is repeated until the desired threshold is reached.

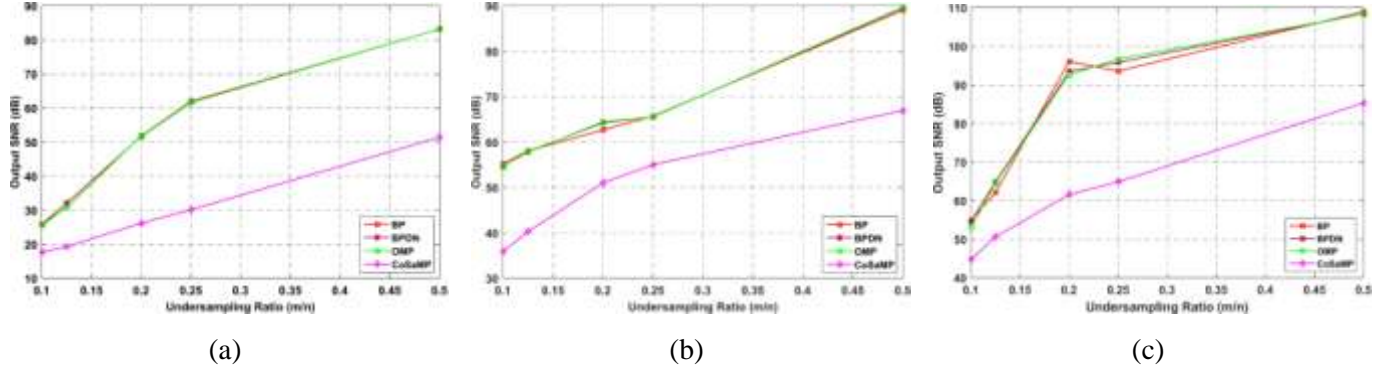


Figure. 8. Performance comparison of CS reconstruction algorithms for reconstructing different ECG signal data sets, based on variation of output SNR for different values of undersampling ratio: (a) data set 100, (b) data set 108, (c) data set 112.

In this paper, BP and BPDN are implemented using CVX, which is a package for specifying and solving convex programs [26]. The OMP and CoSaMP algorithms are the MATLAB functions available at [27]. As per the previous experimental settings of n , m and φ for an undersampling factor of 2, the size of reconstruction matrix Θ will be 260×520 . Since, $\Theta = \varphi\psi$, so the size of Fourier matrix ψ will be 520×520 . The resulted reconstruction matrix Θ and compressive measurements y are then given as inputs to the reconstruction algorithms. The output of reconstruction algorithms is the sparse estimate \hat{s} , *i.e.*, the frequency spectrum of reconstructed ECG signal in this case. From estimated frequency spectrum, the estimate of signal in time domain, *i.e.*, \hat{x} is obtained by taking its inverse Fourier transform. The reconstruction results for ECG signal which is taken from data set 100 by these four methods are shown in Fig.5. Similarly, the reconstruction results for data sets 108 and 112 are shown in Fig.6 and Fig.7, respectively.

C. Reconstruction Performance Comparison

The performance of CS reconstruction methods is compared to identify the better performing algorithm for reconstructing ECG signal back from compressive measurements. For this, the reconstruction is performed for different undersampling ratios on all ECG signals. The output SNR is calculated for different values of undersampling ratios, (m/n) , as per (14). The resulted variations of output SNR with undersampling ratio, are shown in Fig.8(a), Fig.8(b) and Fig.8(c), corresponding to the ECG data sets 100, 108 and 112 respectively. In highly undersampled cases as well, the algorithms are able to achieve sufficient output SNR for data sets 108 and 112. The output SNR increases as the undersampling ratio increases. The maximum output SNR achieved are 83.20, 89.71 and 109 dB respectively for the three datasets. Here, one point to note is that the undersampling ratio and undersampling factor are inverse of each other. Another point is that the performance of OMP and CoSaMP algorithms is dependent on sparsity parameter k .

$$\text{Output SNR} = 20 \log_{10} \frac{\|s\|_2}{\|s - \hat{s}\|_2}. \quad (14)$$

The comparison of performance of these algorithms for the three data sets is summarized in Table III. The comparison has been done on the bases of speed, undersampling ratio and accuracy of reconstruction. It has been observed that the convex optimization, which is a global optimization method, is slower than the greedy approach. Therefore, the algorithms BP and BPDN are highly complex and converges slowly.

TABLE III. Performance Comparison of CS Reconstruction Algorithms for Different Data Sets.

Data Set	Algorithm	Speed (s)	No. of iterations	max. output SNR (dB)
100	BP	3.501178	12	83.17
	BPDN	4.278765	12	83.20
	OMP	0.621551	260	83.18
	CoSaMP	0.104887	2	51.41
108	BP	3.498982	12	89.06
	BPDN	4.580422	14	89.55
	OMP	0.769599	260	89.71
	CoSaMP	0.188566	2	66.96
112	BP	3.772987	13	109
	BPDN	4.030914	11	108.42
	OMP	0.634333	260	108.37
	CoSaMP	0.128850	3	85.32

On the other hand, the algorithms OMP and CoSaMP are simpler and converges rapidly. As far as the reconstruction speed is concerned, CoSaMP, which is a parallel greedy approach, is fastest of four and converges in fewer iterations compared to the other algorithms. On the other hand, the algorithms BP, BPDN and OMP have comparable SNR values and outperforms CoSaMP. The iteration count of OMP is the highest, but due to its simpler operation it takes lesser time. As, overall performance of OMP is optimal, therefore, in this paper, OMP will be used for further processing of all ECG signal data sets.

V. Proposed Feature Extraction Algorithm And Disease Classification

A. Feature Extraction

The features are extracted from ECG signal for classifying the diseases indicated by the signal. The basic pattern of electrical activity across the heart is shown in Fig.9. This depicts the important features of ECG signal that needs to be extracted, like, R-peak, Q and S-minimas, etc. For extracting features from ECG signal, a novel feature extraction algorithm is proposed in this paper. The main steps of this algorithm are shown by the flow chart in Fig.10 and are described below. The applicability of this algorithm has been checked for several ECG data sets to validates its universality for ECG signals. The features are extracted from original ECG signal, as well as from the CS reconstructed ECG signals for different undersampling factors, for the purpose of comparison.

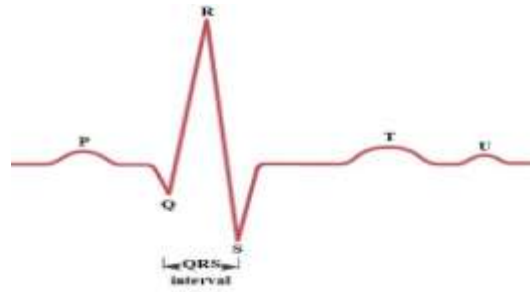


Figure. 9. Representation of basic pattern of electrical activity across heart depicting its main features.

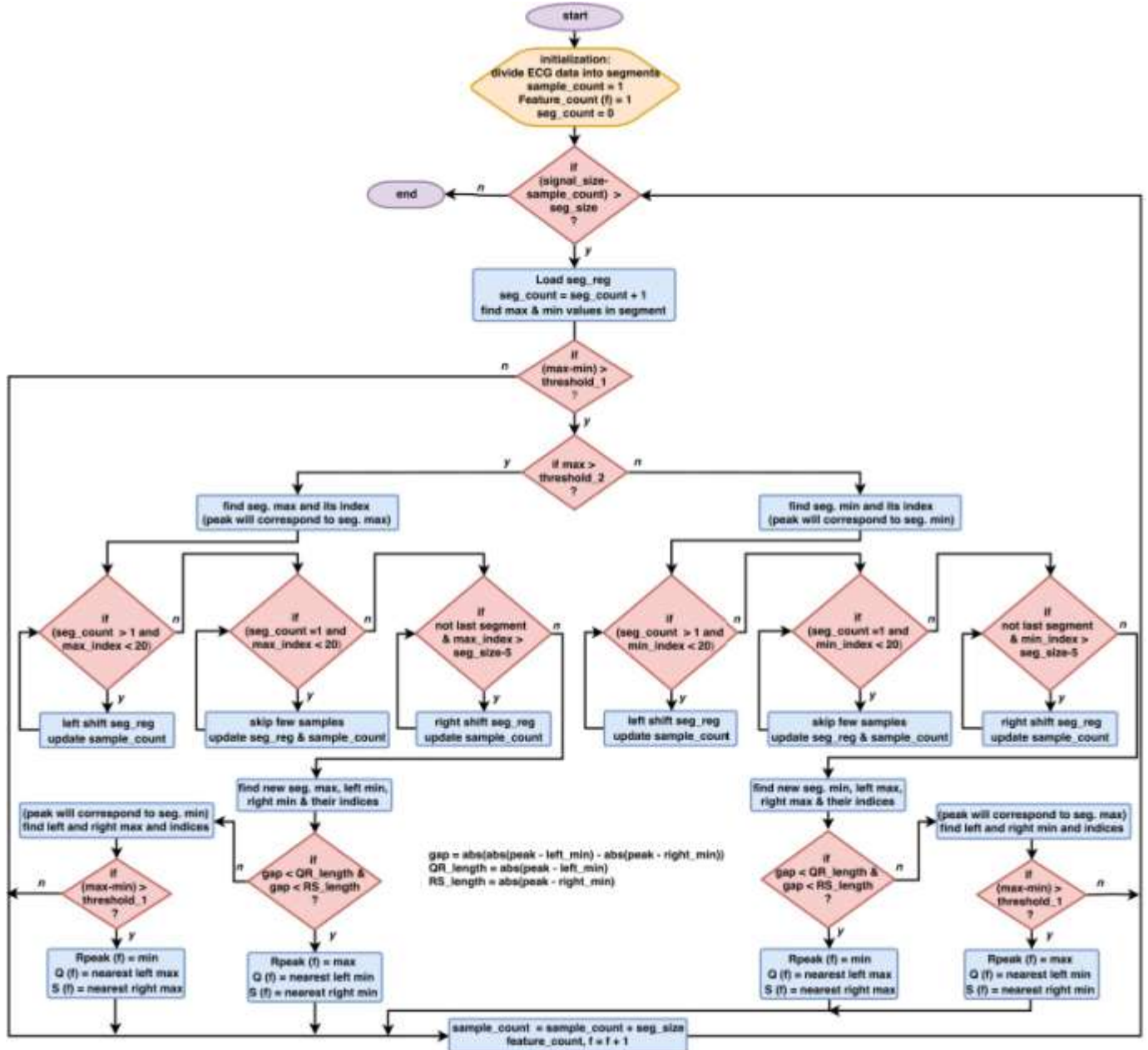


Figure. 10. ECG feature extraction process flow.

TABLE IV. Comparison of Extracted ECG Features from CS Reconstructed Signal for Different Undersampling Factors with Features Extracted from Original Signal

ECG signal type		data set 100		data set 108		data set 112	
		QRS width	Heart Rate	QRS width	Heart Rate	QRS width	Heart Rate
Original		0.0530	73.71	0.117	61.92	0.058	82.08
CS Reconstructed ECG signal with undersampling factor	2	0.0530	73.71	0.103	62.11	0.067	82.08
	4	0.0530	73.71	0.109	62.11	0.07	82.08
	8	0.0640	74.53	0.108	62.24	0.075	82.08
	10	0.0940	73.80	0.131	62.24	0.078	82.42

TABLE V. Performance Comparison of R-Peak Detection Rate.

Method	R-peak detection rate
Proposed	100%
Hilbert transform [28]	99.61%
Hilbert and wavelet transform [29]	98.31%
Haar wavelet transform [30]	99.46%
Wavelet transform [31]	99.59%

- *R-Peak Identification:* The features are extracted from ECG data by first dividing it into segments and then detecting the R-peaks segment wise. For this, segment maxima and minima are obtained. The segment maxima is first tested for positive or negative, which discriminates whether the signal is of type 100, *i.e.*, erected with positive peak or 108/112, *i.e.*, inverted/erected with negative peak. In case the ECG signal is of type 100 and if the signal height between maxima and adjacent minima is greater than threshold_1 then that maxima will be considered as R-peak. In case of signal type 108, minima will qualify for R-peak, while in case of type 112 a negative maxima has to be selected as R-peak. The R-peaks detected in case of ECG data set 100 are shown in Fig.11.
- *QRS-Complex Identification:* In case of ECG data sets 100 and 112, after R-peak detection, its adjacent left and right minimas are detected. If the signal height between maxima and these minimas is greater than threshold_2 then these left and right minimas will be considered as Q and S minimas, respectively. Now, after detecting the Q and S minimas, the width of QRS-complex is calculated for that particular segment of the ECG signal. In case of ECG signal type 108, left and right adjacent maximas has to be detected for Q and S.
- *Heart Rate:* Disease classification requires two main features: i). the width of QRS-complexes and ii). heart rate. The heart rate can be calculated as per equation (15), where, RR-interval is the interval between two R-peaks.

$$\text{Heart Rate, } \square\square = \frac{60}{\text{RR-interval}} \text{ bpm} \quad (15)$$

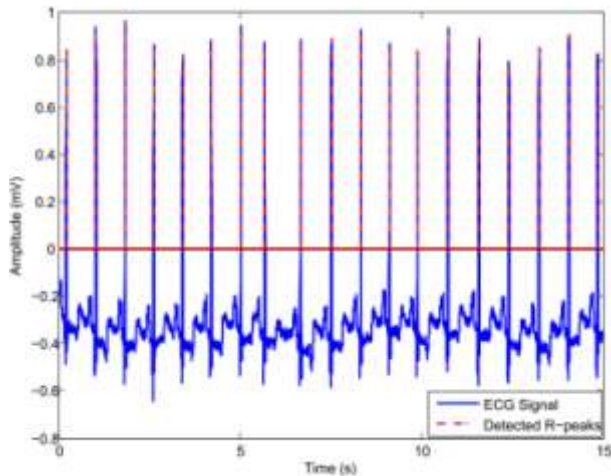


Figure. 11. The R-peaks detected for ECG signal taken from data set 100.

The process is repeated for all the segments. The features extracted from original ECG signal and OMP reconstructed signals for different undersampling factors are shown in Table IV. The features obtained from CS reconstructed output are found to be comparable to the features extracted from original ECG signal. Also, as the CS undersampling is increased, the change in heart rate is not so significant, which is within acceptable range. Similarly, The QRS width also increases as the undersampling is increased and reaches the upper limit for undersampling factor of 10. If the CS undersampling factor is further increased, then the resulted features are no longer acceptable. A comparison of R-peak detection rate is shown in Table V. The proposed algorithm is able to detect all the R-peaks exactly with an 100% detection rate, compared to other methods.

TABLE VI. ECG Feature Constraints for Disease Classification.

Feature Constraints	Disease
QRS-width > 0.14	Right Bundle Branch Block
HR < 50	Bradycardia
HR > 100 and QRS-width > 0.12	Ventricular Tachycardia
< 60 HR < 100 and 0.04 < QRS-width < 0.10	Normal Functioning
0.10 < QRS-width < 0.12	Incomplete Bundle Branch Block
QRS-width > 0.12	Bundle Branch Block

B. Disease Classification

The disease classification has been done based on following observations: if QRS-width > 0.14, then disease is right bundle branch block. If HR < 50 then disease is bradycardia. If HR > 100 and QRS-width > 0.12, then disease is ventricular tachycardia. If HR is in between 60 to 100 and QRS-width is in between 0.04 to 0.10, then heart functioning is normal. If QRS-width is in between 0.10 to 0.12, then disease is incomplete bundle branch block. If QRS-width > 0.12, then disease is bundle branch block [20]–[24]. A summary of ECG feature constraints for disease classification is presented in Table VI.

Based on these constraints, the disease status has been computed corresponding to the features presented in Table IV. The disease status so obtained is given in Table VII.

TABLE VII. Comparison of Disease Status of Original ECG Signal and CS Reconstructed Signals for Different Undersampling Factors.

ECG signal type		Disease Status		
		data set 100	data set 108	data set 112
Original		Normal	Incomplete Bundle Branch Block	Normal
CS Reconstructed ECG signal with undersampling factor	2	Normal	Incomplete Bundle Branch Block	Normal
	4	Normal	Incomplete Bundle Branch Block	Normal
	8	Normal	Incomplete Bundle Branch Block	Normal
	10	Normal	Bundle Branch Block	Normal

VI. Robustness Analysis of Compressive Sensing

A further investigation has been done along with the results presented in previous sections to check the robustness of CS for ECG monitoring. Mainly, two aspects of CS, denoising and information security have been studied, as presented below:

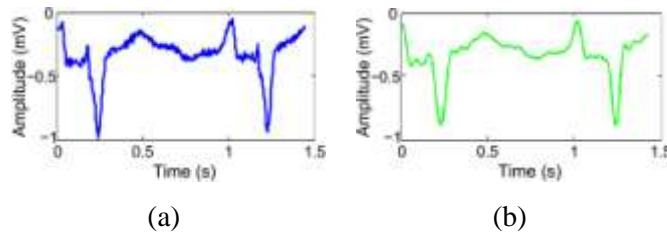


Figure. 12. Analysis of denoising aspect of CS: (a) original ECG signal from data set 108, (b) denoised signal obtained from CS reconstruction using OMP for an undersampling factor of 16.

1) *Denoising Effect:* To analyse denoising effect of CS, the ECG data set 108 has been chosen, as it is a noisy ECG signal. The denoising effect has been observed in the CS reconstructed output, as the undersampling factor is increased. The output reconstructed by OMP for an undersampling factor of 16 is shown in Fig.12(b), which clearly indicates the denoising effect of CS.

2) *Information Security Feature:* The information security feature of CS has also been analysed in case of ECG signal reconstruction. For this, the measurement matrix has been used as a secret key and compressive measurements as encrypted message. First of all, a measurement matrix is formed, which uses a pseudorandom sequence generated for a particular seed, refer section III. Using this measurement matrix, compressive measurements have been generated. Now, the reconstruction is tried using other matrices, which are formed using pseudorandom sequences generated for all other possible seeds. It has been observed that none of the matrices are able to reconstruct the original signal back. This verifies the information security aspect of CS.

VII. Conclusion And Future Scope

Sampling sparse signals using traditional method is power consuming. CS is a newer sensing paradigm that works well for sparse signal processing and saves power by performing compression at the time of sensing. CS works by randomly sampling at a rate proportional to the sparsity of the underlying signal. There are wide variety of signal processing areas where CS has been used. In this paper, CS has been applied to ECG monitoring. The acquisition of ECG signal is performed via RD technique of CS. For reconstructing original signals back from compressive measurements, two popular CS approaches, namely, convex optimization and greedy approach have been used.

A performance comparison of these approaches shows that as far as reconstruction speed and output SNR are concerned, OMP is better suited for ECG signal reconstruction, compared to BP, BPDN and CoSaMP. Then, features are extracted from original and CS reconstructed signals, using the proposed feature extraction algorithm. The universality of proposed algorithm has been verified on several ECG data sets taken from MIT-BIH database. The R-peak detection rate obtained using the proposed algorithm is 100%. A comparison of features extracted from the reconstructed signals for various undersampling factors and the original signal has been done. Then from extracted features, the disease classification has been done. Upto an undersampling factor of 10, the obtained results are comparable and proves the applicability of CS for ECG monitoring. Last but not the least, the robustness analysis done on CS reconstructed ECG signals also supports the candidature of CS for ECG monitoring.

The future scope of this paper is to extend this work for real time ECG monitoring using CS. This includes the implementation of this work using suitable hardware platform, so that, the cost and overall performance is optimized and the system can be used for flawless CS based ECG monitoring.

References

- [1] E. J. Candès, J. Romberg and T. Tao, "Robust uncertainty principles: exact signal reconstruction from highly incomplete frequency information," in *IEEE Trans. on Inf. Theory*, vol. 52, no. 2, pp. 489-509, Feb. 2006.
- [2] D. L. Donoho, "Compressed sensing," in *IEEE Trans. on Inf. Theory*, vol. 52, no. 4, pp. 1289-1306, April 2006.
- [3] R. G. Baraniuk, "Compressive Sensing [Lecture Notes]," in *IEEE Signal Process. Mag.*, vol. 24, no. 4, pp. 118-121, July 2007.
- [4] E. J. Candès and M. B. Wakin, "An Introduction to Compressive Sampling," in *IEEE Signal Process. Mag.*, vol. 25, no. 2, pp. 21-30, March 2008.
- [5] R. Baraniuk, M. Davenport, M. Duarte, and C. Hegde. "An Introduction to Compressive Sensing," *OpenStax-CNX*. April 2, 2011. <http://legacy.cnx.org/content/col11133/1.5/>.
- [6] E. J. Candès and J. Romberg, "Sparsity and Incoherence in Compressive Sampling," in *Inverse Problems*, Vol. 23, No. 3, pp. 969-985, 2007.
- [7] G. H. Golub and C. F. Van Loan, "Matrix Analysis" in *Matrix Computations*. 4th Ed., Baltimore, MD: The Johns Hopkins University Press, 2013, ch.2, pp. 68-73.
- [8] G. Strang, "Linear Algebra and Its Applications", 4th Ed., USA: Thomson on Learning, Inc., 2006.
- [9] D. L. Donoho, "For Most Large Underdetermined Systems of Linear Equations the Minimal L1-norm Solution is also the Sparsest Solution," in *Commun. on Pure and Applied Math.*, vol. 59(6), pp. 797-829, June 2006.
- [10] E. Candès and T. Tao., "Decoding by linear programming," in *IEEE. Trans. Inform. Theory*, vol. 51, no. 12, pp. 4203 - 4215, Dec. 2005.
- [11] M. F. Duarte et al., "Single-pixel imaging via compressive sampling," in *IEEE Signal Process. Mag.*, vol. 25, no. 2, pp. 83-91, March 2008.

- [12]J. A. Tropp, J. N. Laska, M. F. Duarte, J. K. Romberg and R. G. Baraniuk, "Beyond Nyquist: Efficient Sampling of Sparse Bandlimited Signals," in *IEEE Trans. on Inf. Theory*, vol. 56, no. 1, pp. 520-544, Jan. 2010.
- [13]M. Mishali and Y. C. Eldar, "From Theory to Practice: Sub-Nyquist Sampling of Sparse Wideband Analog Signals," in *IEEE Journal of Selected Topics in Signal Process.*, vol. 4, no. 2, pp. 375-391, April 2010.
- [14]J. P. Slavinsky, J. N. Laska, M. A. Davenport and R. G. Baraniuk, "The compressive multiplexer for multi-channel compressive sensing," in *IEEE Int. Conf. Acoust., Speech and Signal Process. (ICASSP)*, Prague, Czech Republic, pp. 3980-3983, 2011.
- [15]M. Rani, S. B. Dhok and R. B. Deshmukh, "A Systematic Review of Compressive Sensing: Concepts, Implementations and Applications," in *IEEE Access*, vol. 6, pp. 4875-4894, Jan. 2018.
- [16]Chen, S., Donoho, D.L., and Saunders, M.A., "Atomic Decomposition by Basis Pursuit," in *SIAM J. Sci Comp.*, vol. 20, no. 1, pp. 33-61, 1999.
- [17]Y. C. Pati, R. Rezaifar and P. S. Krishnaprasad, "Orthogonal matching pursuit: recursive function approximation with applications to wavelet decomposition," in *Proc. 27th Asilomar Conf. Signals, Sys. and Computers*, Pacific Grove, CA, vol. .1, pp. 40-44, 1993.
- [18]D. Needell and J. Tropp, "CoSaMP: Iterative signal recovery from incomplete and inaccurate samples," in *Appl. Comput. Harmon. Anal.*, vol. 26, no. 3, pp. 301-321, May 2009.
- [19]W. Yin, S. Morgan, J. Yang and Y. Zhang, "Practical compressive sensing with Toeplitz and circulant matrices," in *Visual Comm. and Image Process.*, 2010.
- [20]B. Zhou, Q. Ma, Y. Song and C. Bian, "Cloud-based dynamic electrocardiogram monitoring and analysis system," in *9th International Congress on Image and Signal Processing, BioMedical Engineering and Informatics (CISP-BMEI)*, Datong, pp. 1737-1741, 2016.
- [21]P. Sahoo, H. Thakkar and M. Lee, "A Cardiac Early Warning System with Multi Channel SCG and ECG Monitoring for Mobile Health," in *Sensors*, vol. 17, no. 4, pp. 711, 2017.
- [22]A. Dixon, E. Allstot, D. Gangopadhyay and D. Allstot, "Compressed Sensing System Considerations for ECG and EMG Wireless Biosensors," in *IEEE Transactions on Biomedical Circuits and Systems*, vol. 6, no. 2, pp. 156-166, 2012.
- [23]Kai XU, Yuhao Wang, Yixing Li, Fengbo Ren, "A Data-Driven Compressive Sensing Framework for Long-Term Health Monitoring," available online at *arXiv:1606.01872v1 [cs.IT]*, Jun 2016.
- [24]M. Abo-Zahhad, A. Hussein and A. Mohamed, "Compression of ECG Signal Based on Compressive Sensing and the Extraction of Significant Features," in *Int. J. Comm., Network and Sys. Sciences*, vol. 08, no. 05, pp. 97-117, 2015.
- [25]G. Moody *et al.*, "The impact of the MIT-BIH Arrhythmia Database," in *IEEE Eng. Med. and Biol.*, vol. 20, no. 3, pp. 45-50, May. 2001.
- [26]M. Grant and S. Boyd, CVX: Matlab software for disciplined convex programming, version 2.0 beta, September 2013. <http://cvxr.com/cvx>
- [27]S. Becker, A matlab function: CoSaMP and OMP for sparse recovery, ver. 1.7, Aug 2016. [online] <https://in.mathworks.com/matlabcentral/fileexchange/32402-cosampand-omp-for-sparse-recovery>
- [28]D. Benitez, *et al.*, "The use of the Hilbert transform in ECG signal analysis," in *Comput Biol Med.*, vol. 31, pp. 399-406, 2001.
- [29]JPV. Madeiro, *et al.*, "An innovative approach of QRS segmentation based on first-derivative, Hilbert and Wavelet Transforms," in *Med Eng Phys.*, vol. 34, pp. 1236-1246, 2012.
- [30]Z. Zidelmal, *et al.*, "QRS detection based on wavelet coefficients," in *Comput Methods Prog Biomed.*, vol. 107, pp. 490-496, 2012.
- [31]M. Faezipour, *et al.*, "A patient adaptive profiling scheme for ECG beat classification," in *IEEE Trans Inform Technol Biomed.*, vol. 14, pp. 11531165, 2010.